

## Statistical Description of the Uniaxial Creep Behavior of Polypropylene Foam

JAY K. LEPPER and NORRISS W. HETHERINGTON,  
*Lawrence Radiation Laboratory, University of California,  
Livermore, California 94550*

### Synopsis

The basis of a statistical method for the analysis of creep data is described. The method consists of response surface fitting to a Taylor series expansion of a function about a point. The method is capable of treating multiaxial stress data and includes other variables, such as temperature, without undue mathematical complications. In addition, the statistical approach can account for such things as experimental error and sample variation. The uniaxial compressive creep-recovery behavior of a newly developed polypropylene foam was measured under loads of 140-705 g./cm.<sup>2</sup> and temperatures of 23-74°C. The foam has a nominal density of 0.07 g./cc. and a mean molecular weight between crosslinks of 10,000. The creep behavior is described by a Taylor series expansion through the second order of a function of applied load, test temperature, foam density, and log time.

### INTRODUCTION

This report partially describes the compressive creep-recovery behavior of a polypropylene plastic foam.

Polypropylene foams (PPF) are relative newcomers to the line of commercially available plastic foams. Polyethylene foams have been available for a number of years, but have had serious limitations. Conventional (low-density) polyethylene shows serious loss of mechanical properties at elevated temperature. Attempts to overcome this by crosslinking the foam have been unsuccessful. Linear high-density polyethylene has higher temperature resistance and can be more reliably crosslinked, but it has not been successfully foamed except in thin sheets. Polypropylene appears to be more uniformly foamable than either type of polyethylene and offers desirable properties. Polypropylene ( $T_g \approx -18^\circ\text{C}.$ ) has higher temperature resistance than polyethylene ( $T_g \approx -120^\circ\text{C}.$ ) and can be crosslinked. The new PPF materials are produced commercially in thicknesses up to 1 in. and offer the desirable chemical properties of a polyolefin combined with physical properties potentially superior to those of the polyethylenes.

Foam plastics in structural applications can be expected to support a load for long periods of time and at elevated temperatures. For that

reason, it is important to know the time-temperature behavior of the foam. From a knowledge of the behavior of the polypropylene polymer at elevated temperature, it is anticipated that the PPF would exhibit desirable behavior under loads for extended periods of time at elevated temperature. The actual time-temperature behavior of the PPF was not known and there is no known way to predict the properties of the foam from the properties of the polymer.

The creep-recovery behavior of a material is one measure of its time-temperature response. Foam materials in structural applications are most generally under a compressive or shear load. We have investigated the compressive creep-recovery behavior of one polypropylene foam. This material is manufactured by a proprietary process, and complete characterization is not available.

## PROCEDURE

### Material Description

The material tested in this investigation was a polypropylene foam manufactured by Haveg Industries and designated as Minicel PPF-5UM. This material was supplied in sheets of 2.54-cm. (1-in.) thickness and with a nominal density of 0.07 g./cc. Within our measuring precision of  $\pm 0.002$  g./cc. on samples approximately 16 cc. in volume, the foam was uniform in density. The cell structure was fine and uniform with irregular dodecahedral cells approximately 200  $\mu$  in major dimension. Air pycnometer measurements indicated the foam was essentially 100% closed cell. The foam was 92% cell volume and 8% cell wall. The only irregularities observed in the cell structure appeared to be small areas of polymer (gel) that were incompletely foamed. These areas appeared to swell and become visually more pronounced after the foam had been oven aged at 100°C.

TABLE I  
Typical Chemical Analysis of Polypropylene Foam

Element	Content	
	wt.-%	ppm
C	82.38	
H	14.08	
N <sup>a</sup>	2.15	
S	0.063	
Al		500
Ca		500
Fe		750
Mg		2500
Si		5000
Ti		150
Ash (total)	3.5	

<sup>a</sup> Includes gas in cell (if air, 1.3% N<sub>2</sub>; if N<sub>2</sub> blown, 1.7% N<sub>2</sub>).

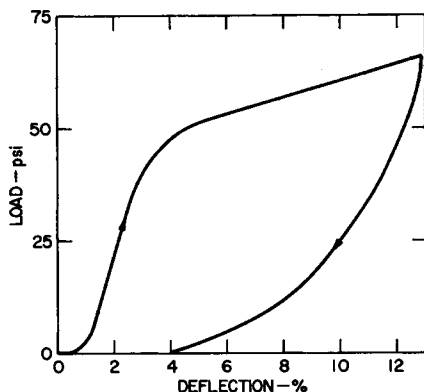


Fig. 1. Typical load-deflection curve for polypropylene foam at 23°C. Test conditions: compression; crosshead velocity, 0.05 in./min.; foam density, 0.07 g./cc.

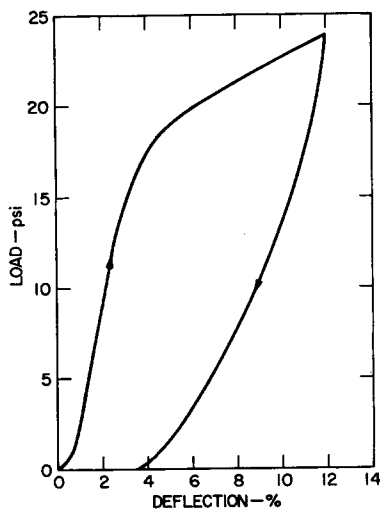


Fig. 2. Typical load-deflection curve for polypropylene foam at 100°C. Test conditions: compression; crosshead velocity, 0.05 in./min.; foam density, 0.07 g./cc.

Solvent swelling tests indicated that the foam was highly crosslinked and that crosslinking was uniform through a slab of the foam. The molecular weight between crosslinks ( $M_c$ ) calculated from the Flory-Huggins solvent swelling relationship was 12,000 for samples that showed no gel inclusions.<sup>1</sup> This value for  $M_c$  corresponds to 10.5% by weight extractables in toluene. Samples that showed gel inclusions gave a molecular weight between crosslinks of 15,000 with 12.5% by weight extractables. This small variation in  $M_c$  was not significant but might be expected to reoccur because the swollen foam volumes were approximately double for samples with gel inclusions. Also, the density of samples with gel inclusions decreased ~15% after oven aging at 100°C.

The typical chemical analysis of PPF is given in Table I. Figures 1 and 2 show typical static compressive load-deflection curves measured for foam at 23 and 100°C. Further characterization of the material is not available.

### Test Specimen Preparation

Test specimens for the creep studies were prepared by slicing with a fine-toothed bandsaw pieces  $1\frac{5}{8} \times 1\frac{5}{8} \times \frac{3}{8}$  in. from a slab 1 in. thick. The cut surfaces were smoothed by hand sanding. The bulk densities were determined by weighing and measuring (with a vernier caliper) the specimens.

### Experimental Design

The selection of appropriate experimental designs has been extensively discussed in the literature.<sup>2,3</sup> To study the creep of PPF, we selected a composite design that was developed to explore and to optimize multi-factor relationships of an unknown functional form.<sup>4-7</sup> These designs have been successfully used by the chemical industry in England and by a segment of the rubber and space industry in this country. We have successfully used these designs to investigate injection-molding processes, polystyrene foam production, and the creep behavior of polystyrene foam.<sup>8,9</sup>

The design uses the methodology of surface fitting to investigate the shape of the unknown, but assumed, functional response. We assume only that there is a functional relationship between the independent variables and the response. This function can be approximated by a Taylor series expansion about a point within the design. Using the Taylor series expansion about a point to describe an unknown response function has some serious practical costs and risks. It would be risky to attempt to describe a large surface with too few data or with data poorly located. It is costly to obtain large quantities of data. Prior knowledge of the general shape of the response and the relative importance of the independent variables is integral to the success of the experiment.

From prior knowledge of the creep behavior of plastic foams, we would expect applied load, temperature, humidity, foam density, and time to be the major variables affecting the creep behavior of the foam.<sup>8</sup> Prior knowledge of polypropylene indicated that the humidity would not be a major variable. Within our ability to measure density ( $\pm 0.002$  g./cc.) on samples with a 16-cc. volume, it was determined that the density of the PPF tested was constant. We then assume

$$C = f(\sigma_0, T, t) \quad (1)$$

where  $C$  is some measure of creep, such as creep deflection,  $\sigma_0$  is the applied load,  $T$  is the test temperature, and  $t$  is time. The boundaries of the experiment are established by the domain of the variables in which we are

interested. Previous experience with the creep behavior of plastic foams indicates that the functional relationships between the independent variables and the creep response can be approximated by a Taylor series expansion in the variables through the second order.<sup>8</sup> Hence, we state

$$C = a_0 + a_1\sigma_0 + a_2T + a_3t + a_{11}\sigma_0^2 + a_{22}T^2 + a_{33}t^2 \\ + a_{12}\sigma_0T + a_{13}\sigma_0t + a_{23}Tt \quad (2)$$

The quadratic form forces the response surface to be a limited group of conics. Experience with the physical process of uniaxial creep implies that this restriction is reasonable.

Considering creep as a function of three variables (load, temperature, and time) and testing these variables at five levels would require running a minimum of 20 tests. The chemical structure of polypropylene and a knowledge of the polymer aging characteristics make it appear unlikely that the PPF would age during a 150-hr. test, even in an experiment under the maximum load and temperature of the experiment (705 g./cm.<sup>2</sup> and 75°C.). One creep test can be used to determine deflections at several levels of the time variable. Statistically, this confounds the variations in the creep response caused by time and aging, but allows us to design a creep experiment as a function of two variables (load and temperature) and to run only 12 tests since each creep test includes within it all levels of time.

The selected independent variables are scaled to cover the domain of interest. Scaling requires some judgment of the functional mechanism because it is intended that equal increments of response will be obtained near the center of the domain for unit changes along the scaled variable axes. We proposed to investigate applied loads of 140–705 g./cm.<sup>2</sup>, temperatures of 23–75°C., and times of 0–120 hr.

Previous creep data for silicone foam were very well described by fitting them to

$$\epsilon = a + b \ln t + c(\ln t)^2 + \dots \quad (3)$$

which indicated that creep is a logarithmic function of time.<sup>8</sup> Accordingly, we scale  $\ln t$  from 0.1 to 120 hr. Table II shows the correspondence between the real and scaled variables.

TABLE II  
Correspondence Between Real and Scaled Variables Over the Range Investigated

Real variables						Scaled variables
Load $\sigma_0$		Temperature $T$ , °C.	Time			
psi	g./cm. <sup>2</sup>		$t$ , hr.	$\ln t$		
2.0	141	23	0.1	-2.3026	$-\sqrt{2}$	
3.2	225	30.5	0.3	-1.2646	-1	
6.0	422	48.5	3.5	1.2425	0	
8.8	619	66.5	42.5	3.7496	1	
10.0	704	74	120	4.7875	$\sqrt{2}$	

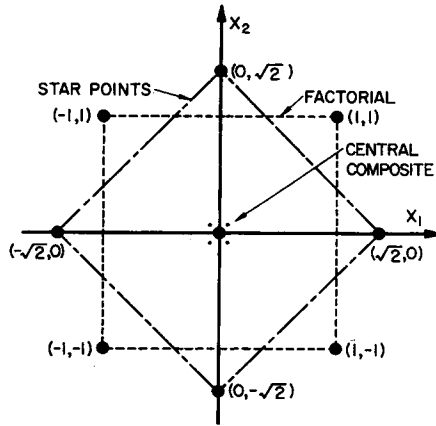


Fig. 3. Composite design for two variables.

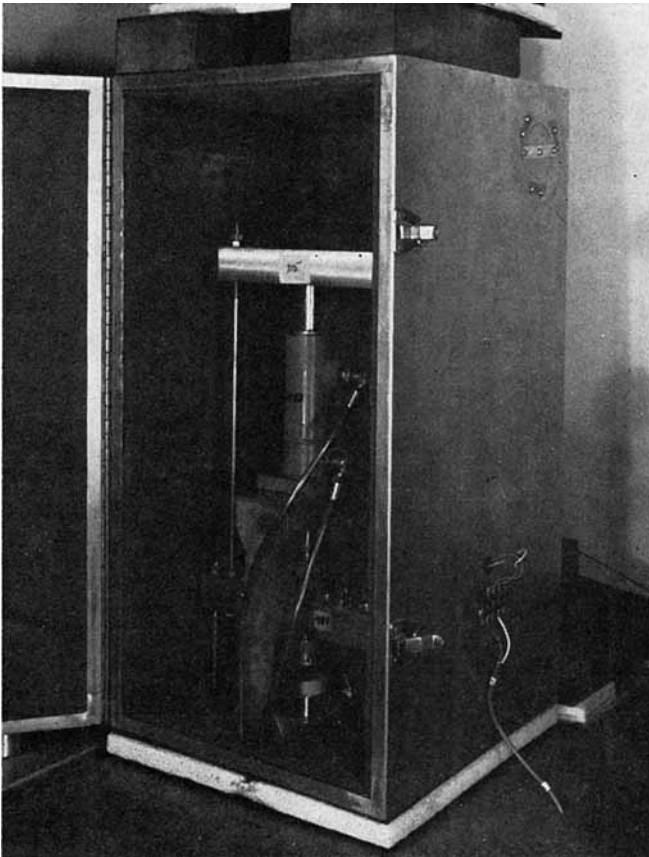


Fig. 4. Compressive creep fixture.

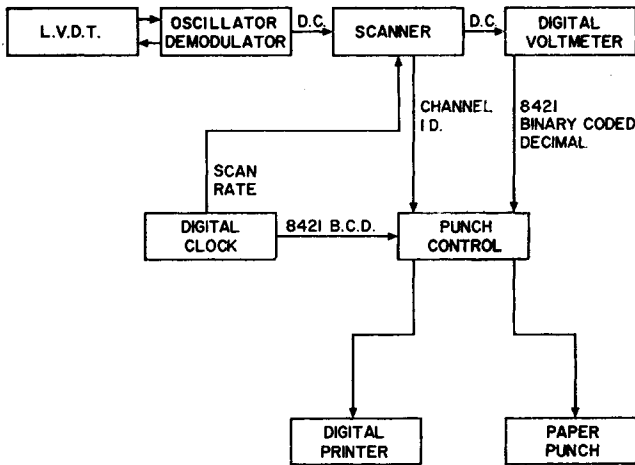


Fig. 5. Schematic of data collection system for creep and recovery experiments.

The design in scaled variables is made orthogonal, rotatable, and blockable. The reasons and advantages of these features are discussed elsewhere<sup>8,10,11</sup> but for clarity are briefly restated here. Making the design orthogonal allows individual estimates of the fitted polynomial coefficients to be made with the minimum constant error due to least-squares fitting. In addition, this feature simplifies the calculations by keeping the error terms on the diagonal of the variance-covariance matrix. This means that the variances are minimum and constant and that the covariances are forced to zero. To make the design orthogonal, the set of comparisons are all independent; the sums of rows are zero and the sums of products of rows by columns are zero, but the vanishing of the product terms does not imply functional independence of the variables. We designed the experiment on a preconceived coordinate system of variables.<sup>12</sup> There may be a simpler, natural variable which controls the process.<sup>13</sup> To describe such a natural variable, it is desirable to translate and rotate (to make canonical) the response surface and retain the same variance. Making the design rotatable provides a spherical variance function for all points in the design. Making the design blockable simply allows it to be extended to evaluate the effects of days, testers, batches, etc. The design is a factorial with central composite points and star points. The factorial feature brings in all combinations of levels for each variable and allows for simplified least-squares curve fitting. The central composite of points gives added weight to these points but provides for an estimate of the experimental error within the scope of the design. The so-called star points make up a second factorial which is rotated in the coordinate system of the design. The added star points provide the additional points to fit the second-order terms which allow for curvature in the response surface. The design used to investigate the creep response of PPF is shown in Figure 3.

The compressive creep testing procedure is routine and was described in previous reports.<sup>8,14</sup> Figure 4 is a photograph of the test fixture, and Figure 5 is a block schematic of the data collection system.

## RESULTS AND DISCUSSION

### Data Treatment

Empirical curve-fitting techniques have been used to treat the compressive creep and recovery data obtained from PPF. The experimental design requires some measure of creep as the response. The PPF data were fitted to a power law,

$$\epsilon = \epsilon_0 + mt^n \quad (4)$$

where  $\epsilon_0$  is in units of strain and  $t$  is in units of time. This form of the equation was selected because it adequately describes the creep behavior of a variety of materials.<sup>14,15</sup> The fitting is done by a least-squares technique, which forces the equation to reflect a physical analogy. The  $\epsilon_0$  is put in units of strain and forced to approximate the elastic response of the material by extrapolating  $\ln \epsilon$  versus  $\ln t$  to  $10^{-4}$  hr., which approximates the loading and unloading times. Then  $m$  and  $n$  are determined by least squares from the equation

$$\ln (\epsilon - \epsilon_0) = \ln m + n \ln t \quad (5)$$

The data to be fitted are sampled uniformly on a log-time scale to avoid weighting the log function being fitted. This is pure curve fitting and the power law is not intended to represent the functional form of the creep mechanism. However, prior experience with this fitting technique has led us to conclude that the constants determined in this manner are measures of creep.<sup>8,14</sup> The exponent of time  $n$  has been particularly useful as a measure of the creep of a material by defining it as a creep "rate"

$$n = \frac{d[\ln (\epsilon - \epsilon_0)]}{d \ln t} \equiv \text{rate} \quad (6)$$

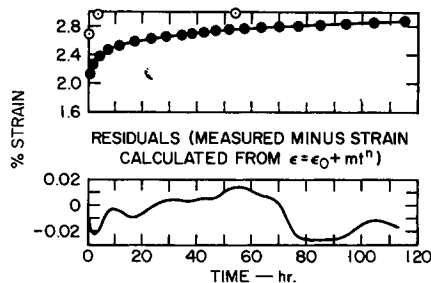


Fig. 6. Data measured for polypropylene foam in creep test 189 at 8.8 psi and 30.5°C.: (●) measured, ungraduated; (—) calculated from  $\epsilon = \epsilon_0 + mt^n$ , ungraduated; (⊙) calculated from  $\epsilon = f(\sigma_0, T, t)$ , graduated.



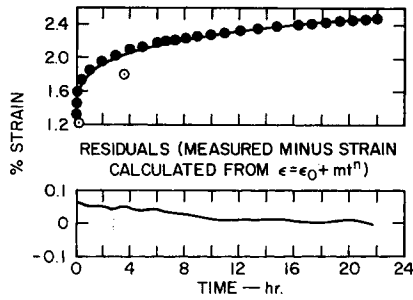


Fig. 7. Data measured for polypropylene foam in recovery test 187 at 6.0 psi and 48.5°C.: (●) measured, ungraduated; (—) calculated from  $\epsilon = \epsilon_0 + mt^n$ , ungraduated; (○) calculated from  $\epsilon = f(\sigma_0, T, t)$ , graduated.

This definition has allowed extrapolations to a first approximation from 100- to 10,000-hr. tests. These extrapolations have been confirmed by 5000-hr. tests.<sup>8</sup>

Figures 6 and 7 show typical creep and recovery data measured for PPF foam. These figures also display the power law fits to the data.

TABLE III  
Analysis of Variance of Creep Deflection Data (Test 189) Fitted by the Power Law,  
 $\epsilon = \epsilon_0 + mt^n$

	Sum of squares $\times 10^{-6}$	Degrees of freedom	Variance $\times 10^{-6}$ <sup>a</sup>
Fit by difference	942	5	188
Residuals $\Sigma(R^2) = \Sigma(X - \hat{X})^2$	1.06	62	0.02
Total $\Sigma(X^2) - n\bar{X}^2$	943	67	14

<sup>a</sup> *F*-ratio of the variances between fit and residuals = 9400.

TABLE IV  
Analysis of Variance of Recovered Deflection Data (Test 187) Fitted by the Power Law,  
 $\epsilon = \epsilon_0 + mt^n$

	Sum of squares $\times 10^{-6}$	Degrees of freedom	Variance $\times 10^{-6}$ <sup>a</sup>
Fit by difference	1386	5	277
Residuals $\Sigma(R^2) = \Sigma(X - \hat{X})^2$	17	80	0.21
Total $\Sigma(X^2) - n\bar{X}^2$	1403	85	16

<sup>a</sup> *F*-ratio of variances between fit and residuals = 1320.

The analysis of variance of creep and recovery for these fits is shown in Tables III and IV, respectively, and indicates that the power law describes the data very well. Table V contains the constants fitted to the 12 tests that made up this experiment. Table V also contains the test conditions of applied load  $\sigma_0$  and test temperature  $T$ . The PPF creep and recovery data have been treated in the same manner.

TABLE V  
 Constants Fitted to  $\epsilon = \epsilon_0 + mt^{n_s}$

Test no.	$\sigma_0$ , g./cm. <sup>2</sup>	$T$ , °C.	Creep			Recovery		
			$\epsilon_0$	$m$	$n$	$\epsilon_0$	$m$	$n$
182	422	23	0.0211	0.0065	0.1111	0.0085	0.0075	-0.1678
183	422	48.5	0.0246	0.0099	0.1163	0.0085	0.0096	-0.1771
184	422	48.5	0.0298	0.0099	0.1129	0.0099	0.0103	-0.1729
185	225	30.5	0.0140	0.0070	0.1167	0.0058	0.0057	-0.1737
186	225	66.5	0.0126	0.0073	0.1236	0.0042	0.0047	-0.1848
187	422	48.5	0.0245	0.0097	0.1148	0.0085	0.0094	-0.1779
188	422	48.5	0.0271	0.0093	0.1120	0.0089	0.0093	-0.1765
189	619	30.5	0.0146	0.0080	0.1200	0.0043	0.0064	-0.1880
190	422	74.0	0.0175	0.0107	0.1266	0.0058	0.0067	-0.1894
191	141	48.5	0.0068	0.0047	0.1284	0.0026	0.0028	-0.1826
192	704	48.5	0.0300	0.0129	0.1158	0.0103	0.0123	-0.1826
193	619	66.5	0.0192	0.0124	0.1281	0.0073	0.0074	-0.1987

• Data were sampled uniformly on  $\ln t$ .

### Data Analysis

The constants shown in Table V give a quick indication that something is wrong. The fits of the  $\epsilon_0$  to the creep data to reflect the initial or elastic deformation do not show the expected increase with the load and temperature. The  $m$  does appear to have an increasing trend with the load and temperature. The  $n$ , which is nearly constant for a material (usually with standard deviations less than 5% of the mean) aside from a stress-temperature dependence, seems to be at two levels, 0.114 and 0.125. These observations lead us to suspect that we were dealing with two populations of data, perhaps a difference in the samples or the testing procedure.

Figures 8 and 9 show  $\epsilon_0$  plotted against  $\ln(\sigma_0 T)$  for creep and recovery, respectively. There appear to be two linear relationships, indicating two populations. The lower values of  $\epsilon_0$  correspond, test for test, with the higher values of  $n$ .

We confirmed, to the best of our ability, that all 12 tests had been run in the same manner; in fact, the tests were run in groups of three so that several were run on the same fixture. There was no correlation between the apparent two populations and the test conditions.

We then examined the specimens, since we suspected a systematic variation. There was a slight difference between the surfaces of the two faces of the specimen that were under load. One surface was fairly smooth and appeared as-molded, whereas the other was slightly rougher from cutting. In addition, there was a slight curvature toward the cut surface. The orientation of the specimen with respect to these surfaces in the creep fixture was recorded, and without exception, those specimens that had been tested with the cut surface toward the upper anvil gave a lower  $\epsilon_0$ . This is not believed to be entirely due to the surface roughness. If we take the initial deflection and subtract the initial recovery, the difference

should, in part, reflect the permanent set or crushing of the surface irregularities. We obtained differences ranging from 0.0023 to 0.0076 in. with no obvious correlation within groups as to orientation in the fixture. There is apparently a tensile force present in the material either as a result of molding or cutting that causes the curvature. This distortion and perhaps the surface condition cause a shift in creep response.

### Elimination of Orientation Variation

The concept of the original experiment design now includes variation due to specimen orientation in the test fixture. This variation was detected because of the relative sizes of the anvils of the test fixture. Because of the shift of creep response related to specimen orientation in the fixture, we had two partial experiments and two populations of material

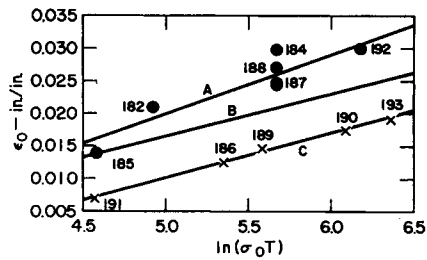


Fig. 8.  $\epsilon_0$  obtained from the fit of creep data to  $\epsilon = \epsilon_0 + mt^n$  plotted against  $\ln(\sigma_0 T)$ : (A) fit of 7 tests, cut surface down; (B) fit of 12 tests, all tests; (C) fit of 5 tests, cut surface up.

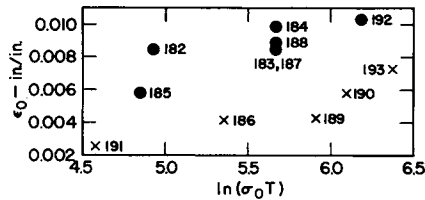


Fig. 9.  $\epsilon_0$  obtained from the fit of recovery data to  $\epsilon = \epsilon_0 + mt^n$  plotted against  $\ln(\sigma_0 T)$ : (●) cut surface down; (×) cut surface up.

behavior. Since there was insufficient material available to complete the design by filling in the missing points of each type, we were faced with the alternatives of abandoning this experiment and repeating it entirely with new materials or of attempting to graduate\* the data and present an approximate picture of the creep behavior of PPF. Since creep tests are, by definition, time consuming and the PPF is a new and interesting material, we chose to attempt both. New samples are being prepared for a repeat experiment. The balance of this report describes the graduating technique used to eliminate concomitant variation and presents data that

\* Transformation of data with a functional relationship.

we think will provide a qualitative description of the creep behavior of PPF.<sup>16</sup>

In Figures 8 and 9 where  $\epsilon_0$  was plotted against  $\ln(\sigma_0 T)$ , we hypothesized that the slope of this plot reflects a material property and that specimen and testing difference is seen as change in intercept. Accordingly, the data were fitted to a linear regression,

$$\epsilon_0 = \bar{\epsilon}_0 + K[\ln(\sigma_0 T) - \overline{\ln(\sigma_0 T)}] \quad (7)$$

where the bars denote the means. The results of this fitting are shown in Tables VI and VII. Test 185 shows some anomaly and accounts for the bulk of the variation of the fit of the tests with the cut surface of the

TABLE VI  
Correlation and Regressions of Creep Data to  $\epsilon_0 = \bar{\epsilon}_0 + K[\ln(\sigma_0 T) - \overline{\ln(\sigma_0 T)}]$   
and  $m = \bar{m} + K[\ln(\sigma_0 T) - \overline{\ln(\sigma_0 T)}]$  which Show High Correlation for the  
Separate Regressions

Fitting $\epsilon_0$	Correlation	Critical value of	Slope K
	coefficient <i>r</i>	correlation coefficient $r_{0.01}$	
All 12 tests	0.568	0.684	0.0071
7 tests with cut surface of specimen down in creep fixture	0.923	0.834	0.0095
5 tests with cut surface of specimen up in creep fixture	0.998	0.917	0.0069
6 tests with cut surface of specimen down in creep fixture (185 deleted)	0.827	0.883	0.0071
Fitting <i>m</i>			
All 12 tests	0.934	0.684	0.0039

TABLE VII  
Correlation and Regressions of Recovery Data to  $\epsilon_0 = \bar{\epsilon}_0 + K[\ln(\sigma_0 T) - \overline{\ln(\sigma_0 T)}]$   
and  $m = \bar{m} + K[\ln(\sigma_0 T) - \overline{\ln(\sigma_0 T)}]$  which Show High Correlation  
for the Separate Regressions

	Fitting $\epsilon_0$			Fitting <i>m</i>	
	Correlation coefficient <i>r</i>	Critical value	Slope K	Correlation coefficient <i>r</i>	Slope K
		of correlation coefficient $r_{0.01}$			
All 12 tests	0.479	0.684	0.0020	0.615	0.0028
7 tests with cut surface of specimen down in creep fixture	0.860	0.834	0.0023	0.976	0.0038
5 tests with cut surface of specimen up in creep fixture	0.971	0.917	0.0025	0.969	0.0026

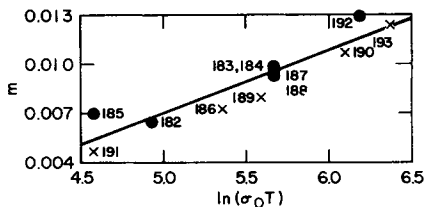


Fig. 10.  $m$  obtained from the fit of creep data to  $\epsilon = \epsilon_0 + mt^n$  plotted against  $\ln(\sigma_0 T)$ : (●) cut surface down; (×) cut surface up.

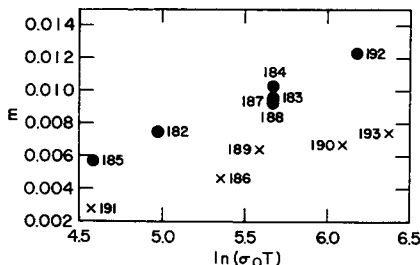


Fig. 11.  $m$  obtained from fit of recovery data to  $\epsilon = \epsilon_0 + mt^n$  plotted against  $\ln(\sigma_0 T)$ : (●) cut surface down; (×) cut surface up.

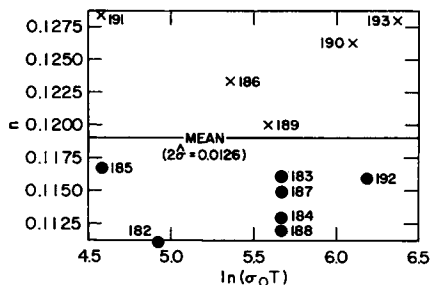


Fig. 12.  $n$  obtained from the fit of creep data to  $\epsilon = \epsilon_0 + mt^n$  plotted against  $\ln(\sigma_0 T)$ : (●) cut surface down; (×) cut surface up.

specimen toward the lower anvil of the test fixture. There were problems with the paper tape punch in the data collection system during this test, so we have discarded test 185 in the second fit shown on Table VI; however, we did not delete this test from the overall analysis. Using a Student  $t$ -test and assuming that the slopes are equal, we found that the difference between the two parallel regressions was significant at the 95% level. The slopes were the same and the intercepts were different according to the orientation of the specimen in the test fixture.

A plot of  $m$  versus  $\ln(\sigma_0 T)$  (Figs. 10 and 11) does not show a separation of data for tests according to the orientation of the specimen in the creep fixture. Values of  $m$  for specimens with the cut surface up appear to be slightly lower, especially in the recovery data. The creep data appear

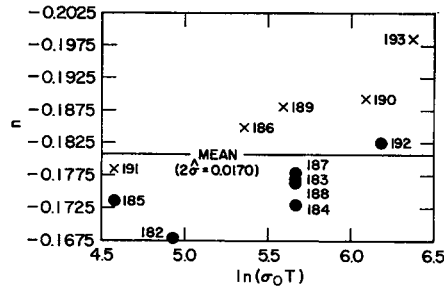


Fig. 13.  $n$  obtained from the fit of recovery data to  $\epsilon = \epsilon_0 + mt^n$  plotted against  $\ln(\sigma_0 T)$ : (●) cut surface down; (×) cut surface up.

to vary within the experimental error as represented by tests 183, 184, 187, and 188. For that reason, the  $m$  of the creep data was assumed independent of the specimen orientation in the fixture. The  $m$  of the recovery data was not independent. The data of both tests were fitted to the linear regression,

$$m = \bar{m} + K[\ln(\sigma_0 T) - \overline{\ln(\sigma_0 T)}] \quad (8)$$

The results of these fits are shown in Tables VI and VII.

Figures 12 and 13 show  $n$  plotted against  $\ln(\sigma_0 T)$ . There is a clear separation between the groups according to whether the cut surface was up or down in the fixture. The magnitude of this separation is small. There is an apparent slope to the data, as would be expected, but tests 185 and 191 do not fit with their respective groups. We could find no explanation for those two tests, so we chose to include them and accept the average  $n = 0.1189$  with a standard deviation of 0.0063 as representing the PPF creep rate. The  $n$  for recovery was  $-0.1806$  with a standard deviation of 0.0085. The standard deviation is 5% of the mean in both cases.

The creep response of PPF of 0.07 g./cc. density tested with applied loads ranging from 140 to 705 g./cm.<sup>2</sup> and temperatures ranging of 23–75°C. can be described by eq. (4) where the constants can be approximated as functions of  $\ln(\sigma_0 T)$ . Therefore, we represent the creep deflection of the material as

$$\epsilon = \bar{\epsilon}_0 + K[\ln(\sigma_0 T) - \overline{\ln(\sigma_0 T)}] + \{\bar{m} + K'[\ln(\sigma_0 T) - \overline{\ln(\sigma_0 T)}]\}t^{\bar{n}} \quad (9)$$

or

$$\epsilon = A \ln(\sigma_0 T) + B + [D \ln(\sigma_0 T) + F]t^{\bar{n}} \quad (10)$$

Equation (10) then was used to graduate the data to eliminate the concomitant variation arising from the specimen orientation in the creep fixture, and to put it in a form suitable for analysis in the original design.<sup>16</sup> These graduated data, as represented by the power law fits, are given in Table VIII.

TABLE VIII  
 Constants for the Power Law,  $\epsilon = \epsilon_0 + mt^n$ , Graduated with Natural  
 Logarithm of the Product of Load and Temperature

Test no.	Creep <sup>a</sup>		Recovery <sup>b</sup>	
	$\epsilon_0$	$m$	$\epsilon_0$	$m$
182	0.0158	0.0067	0.0058	0.0060
183	0.02115	0.0096	0.0073	0.0081
184	0.02115	0.0096	0.0073	0.0081
185	0.01335	0.0053	0.0051	0.0050
186	0.0189	0.0083	0.0067	0.0072
187	0.02115	0.0096	0.0073	0.0081
188	0.02115	0.0096	0.0073	0.0081
189	0.0206	0.0093	0.0072	0.0079
190	0.0242	0.0112	0.0082	0.0093
191	0.0133	0.0053	0.0051	0.0050
192	0.0248	0.0116	0.0084	0.0095
193	0.0261	0.0123	0.0088	0.0100

<sup>a</sup> Average  $n$  for creep was 0.1189.

<sup>b</sup> Average  $n$  for recovery was  $-0.1806$ .

To incorporate the above empirical relationship between  $\epsilon$  and  $\ln(\sigma_0 T)$  into the Taylor series model, we proceed as follows:

$$\epsilon = B + A \ln \sigma_0 + A \ln T + Ft^n + Dt^n \ln \sigma_0 + Dt^n \ln T \quad (11)$$

making the Taylor series expansion in  $\ln \sigma_0$  and  $\ln T$  as

$$\epsilon = a_0 + a_1 \ln \sigma_0 + a_2 \ln t + \dots \quad (12)$$

where

$$a_0 = B + t^n F$$

$$a_1 = a_2 = A + t^n D$$

Having used the power law to describe the data and the log relationship to graduate it, we can surmise that

$$\epsilon = f(\sigma_0 T) + g(\sigma_0 T)t^n \quad (13)$$

The graduated data were fitted to

$$\epsilon = a_0 + a_1 \sigma_0 + a_2 T + a_3 \ln t + \dots \quad (14)$$

through the second order; the coefficients are given in Tables IX and X. Tables IX and X also contain the coefficients of polynomials,

$$\epsilon = a_0 + a_i x_i + a_{ii} x_i^2 \quad (15)$$

fit individually in each of the three variables: load, temperature, and log time. By including the interaction terms in the quadratic, we explain appreciably more of the variation than by using any of the variables singly. The standard deviations of the fits to the polynomials are a full

TABLE IX  
Coefficients for Quadratic and Polynomial Fits to Creep Deflection Data

Coefficient	$f(\sigma_0, T, \tau) \times 10^{-3}$	$f(\tau) \times 10^{-3}$	$f(T) \times 10^{-3}$	$f(\sigma_0) \times 10^{-3}$
$a_0$	32.332	30.635	31.547	32.177
$a_1$	6.398			6.398
$a_2$	4.764		4.764	
$a_3$	3.191	3.190		
$a_{11}$	-1.666			-1.491
$a_{22}$	-1.879		0.546	
$a_{33}$	0.457	0.457		
$a_{12}$	0.027			
$a_{13}$	0.738			
$a_{23}$	0.548			
$\hat{\sigma}$ of fit	0.442	6.87	6.64	5.50
Per cent fit above mean <sup>a</sup>	99			

<sup>a</sup> Per cent fit =  $\{1 - \Sigma(R^2)/[\Sigma(X^2) - n\bar{X}^2]\} 100$ .

TABLE X  
Coefficients for Quadratic and Polynomial Fits to Recovery Deflection Data

Coefficient	$f(\sigma_0, T, \tau) \times 10^{-3}$	$f(\tau) \times 10^{-3}$	$f(T) \times 10^{-3}$	$f(\sigma_0) \times 10^{-3}$
$a_0$	17.562	16.706	18.106	18.843
$a_1$	3.214			3.214
$a_2$	2.390		2.390	
$a_3$	4.500	4.600		
$a_{11}$	-0.842			-0.754
$a_{22}$	-0.442		-0.274	
$a_{33}$	1.016	1.016		
$a_{12}$	-0.002			
$a_{13}$	0.900			
$a_{23}$	0.667			
$\hat{\sigma}$ of fit	0.3610	3.587	6.012	5.711
Per cent fit above mean <sup>a</sup>	99			

<sup>a</sup> Per cent fit =  $\{1 - \Sigma(R^2)/[\Sigma(X^2) - n\bar{X}^2]\} 100$ .

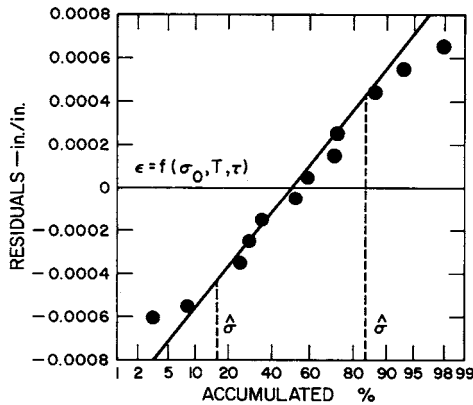


Fig. 14. Residuals from the fit of creep data to  $\epsilon = f(\sigma_0, T, \tau)$  plotted against accumulated %.



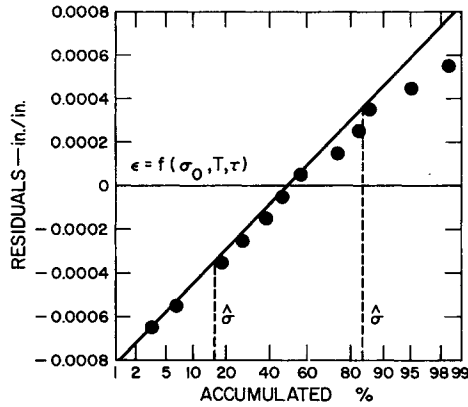


Fig. 15. Residual from the fit of recovery data to  $\epsilon = f(\sigma_0, T, \tau)$  plotted against accumulated %.

order of magnitude higher than the standard deviation of the quadratic fit. Figures 14 and 15 show the residuals about the quadratic fit as normally distributed. The analyses of variance given in Tables XI and XII indicates that the Taylor series model is adequate for describing the creep-recovery behavior of PPF. The residuals are smaller than the testing

TABLE XI

Analysis of Variance of Quadratic Fit of Creep Deflection as a Function of Applied Load, Test Temperature, and ln Time

	Sum of squares $\times 10^{-6}$	Degrees of freedom	Variance $\times 10^{-6}$ <sup>a</sup>
Fit by difference	3424.2	9	380.4
Residuals $\Sigma(R^2)$	9.8	47	0.2
Estimate of error <sup>b</sup> $\Sigma(X_{ctr}^2)$			
$-n_{ctr}\bar{X}_{ctr}^2$	17.9	3	5.9
Total $\Sigma(X^2) - n\bar{X}^2$	3434	59	58.2

<sup>a</sup>  $F$ -ratio of variances between fit and error = 64.47.

<sup>b</sup> Calculated from measured data of four center (ctr) points: tests 183, 184, 187, 188.

TABLE XII

Analysis of Variance of Quadratic Fit of Recovered Deflection as a Function of Applied Load, Test Temperature, and ln Time

	Sum of squares $\times 10^{-6}$	Degrees of freedom	Variance $\times 10^{-6}$ <sup>a</sup>
Fit by difference	2256	9	251
Residuals $\Sigma(R^2)$	6.5	47	0.14
Estimate of error <sup>b</sup> $\Sigma(X_{ctr}^2)$			
$-n_{ctr}\bar{X}_{ctr}^2$	0.3	3	0.1
Total $\Sigma(X^2) - n\bar{X}^2$	2262	59	38

<sup>a</sup>  $F$ -ratio of variances between fit and residuals = 1793.

<sup>b</sup> Calculated from measured data of four center (ctr) points: tests 183, 184, 187, 188.

error. The indication is that the quadratic is close to the functional form of the creep and recovery mechanisms. Creep deflection points calculated from the quadratic equation without graduation are shown in Figure 6.

### SUMMARY AND CONCLUSIONS

The compressive creep-recovery behavior of a crosslinked polypropylene foam (density of 0.07 g./cc.) manufactured by Havg Industries was investigated. Curve-fitting techniques and parametric treatments were used for data reduction and for obtaining correlations between the creep-recovery response of the foam and the test conditions.

The creep-recovery properties of the polypropylene foam were studied at loads of 140–705 g./cm.<sup>2</sup> (2–10 psi) and temperatures of 23–75°C. (73–167°F.). Under conditions of constant load and temperature, both creep and recovery can be described by a power law in time,

$$\epsilon = \epsilon_0 + mt^n$$

The exponent  $n$  has been defined as the creep or recovery rate of the material:

$$n = \frac{d [\ln (\epsilon - \epsilon_0)]}{d \ln t} \equiv \text{rate}$$

The creep rate for the polypropylene foam over the range of loads and temperatures tested was 0.1189. The comparable recovery rate was -0.1806.

The creep and recovery deflections  $(\epsilon_0)_t$  at constant time were linearly related to the logarithm of the product of the load  $\sigma_0$  and temperature  $T$ :

$$(\epsilon_0)_t = (\bar{\epsilon}_0)_t + K[\ln (\sigma_0 T) - \overline{\ln (\sigma_0 T)}]$$

where  $\overline{\ln (\sigma_0 T)}$  and  $(\bar{\epsilon}_0)_t$  are the mean values.

The creep and recovery deflections of polypropylene foam can be described by a Taylor series expansion through the second-order terms of a function of temperature, applied load, and the natural logarithm of time. The ability of the truncated Taylor series to describe the relationship between creep recovery and the three variables, load  $\sigma_0$ , temperature  $T$ , and log time ( $\tau$ ), indicates that a quadratic form adequately describes the function:

$$10^6 \times (\text{creep deflection, } \%) = -16645 + 6\sigma_0 + 809T - 151\tau \\ - 0.04\sigma_0^2 - 6T^2 + 70\tau^2 + 0.008\sigma_0 T + 1.5\sigma_0\tau + 12T\tau \quad (16)$$

$$10^6 \times (\text{recovery deflection, } \%) = -19868 + 55\sigma_0 + 964T - 119\tau \\ - 0.02\sigma_0^2 - 1.4T^2 + 156\tau^2 - 0.006\sigma_0 T + 2\sigma_0\tau + 14.5T\tau \quad (17)$$

where  $\sigma_0$  is applied load,  $T$  is test temperature, and  $\tau$  is ln time (hr.).

To illustrate the typical creep-recovery response of the PPF tested, some typical values were computed from the quadratic fit. The creep deflection of PPF (density 0.07 g./cc.) under an applied load of 422 g./cm.<sup>2</sup> (6 psi) and 23°C. would be 2.2% after 3.5 hr. and 2.6% after 120 hr. If the specimen of PPF were abruptly unloaded after 120 hr., it would recover after 42.5 hr. to 99.2% of its original thickness or about 70% of the creep deflection. If the same 442-g./cm.<sup>2</sup> load were used but the temperature were increased to 75°C., the resulting creep deflection would be 3.5% at 3.5 hr. and 4.2% at 120 hr. If this specimen were abruptly unloaded, it would recover in 42.5 hr. to 98.4% of its original thickness or approximately 63% of the creep deflection. A portion of the unrecovered deflection may be accounted for by the surface condition of the specimen.

## APPENDIX

### Test Procedure and Data Collection

The steps of the creep test procedure are outlined below.

- (1) Measure the dimension and density of the specimen.
- (2) Calibrate the creep fixture; the linearly variable differential transformer (LVDT) is calibrated over its full travel external to the fixture.
- (3) Equilibrate (1 hr. based on measurements from thermocouples buried in typical creep specimens) the creep fixture and specimen at the desired temperature; the laboratory environment is maintained at  $50 \pm 1\%$  relative humidity so the moisture content of the test atmosphere is known.
- (4) Start the data collection system.
- (5) Load the specimen.
- (6) Record deflection-time data.
- (7) Unload the specimen.
- (8) Record deflection-time data.
- (9) Confirm creep fixture calibration.

The data are recorded in 8-4-2-1 binary coded decimal on punched paper tape. The punched paper tape is processed on a PDP-1 computer which associates a time word with a data word and identifies them by channel (test) number. The output of the PDP-1 is punched IBM cards with time-volts in a 6E12.6 format identified by channel number. The cards are sorted by channel number and a deck is assembled for each test. The decks can be processed through an IBM 7094 cathode-ray tube (CRT) routine that will display the data and allow a visual check that the test is running satisfactorily. When the test is complete, the IBM 1401 is used to transfer card images to magnetic tape and all further processing is done on magnetic tape. Further processing of the data on the IBM 7094 is: (1) data are checked to insure proper recording, i.e., sign, exponent, identification, etc.; (2) the time recorded as day-hour-minute-second is converted to decimal, and the voltage recorded from the LVDT

is converted to strain; (3) the creep and recovery portion of a test are separated. The final sorted and converted data are recorded on a library tape on the IBM 1401.

The authors wish to acknowledge the assistance of H. George Hammon and John E. Doig for specimen preparation and characterization; M. Zaslavsky, H. Bechtholdt, and M. E. Reitz for testing; and Paul R. Thompson, Jr. and T. Freeman for computer programming.

This work was performed under the auspices of the U. S. Atomic Energy Commission.

### References

1. P. J. Flory, *Principles of Polymer Chemistry*, Cornell Univ. Press, Ithaca, N. Y., 1953.
2. R. A. Fisher, *The Design of Experiments*, 6th Ed., Oliver and Boyd, London-Edinburgh, 1951.
3. J. Mandel, *The Statistical Analysis of Experimental Data*, Wiley, New York, 1964.
4. G. E. P. Box and K. B. Wilson, *J. Roy. Statist. Soc.*, **B13**, 1 (1951).
5. G. E. P. Box and J. S. Hunter, *Ann. Math. Statist.*, **28**, 195 (1957).
6. G. E. P. Box, *Appl. Statist.*, **6**, 81 (1957).
7. G. E. P. Box and P. V. Youle, *Biometrics*, **11**, 287 (1955).
8. J. K. Lepper, H. G. Hammon, and P. R. Thompson, Jr., "Creep Properties of Polystyrene Bead Foams," Lawrence Radiation Laboratory, Livermore, California, UCRL-14919 (1966).
9. N. W. Hetherington and L. E. Peck, private communication.
10. G. E. P. Box and N. R. Draper, *J. Am. Statist. Assoc.*, **54**, 622 (1959).
11. G. E. P. Box, *Biometrika*, **50**, 335 (1953).
12. G. E. Box, *Bull. Intern. Statist. Inst.*, **38**, 339 (1961).
13. G. E. P. Box, *Bull. Intern. Statist. Inst.*, **36**, 215 (1958).
14. J. K. Lepper and R. L. Jackson, "Compressive Creep of Cushioning Materials," Lawrence Radiation Laboratory, Livermore, California, UCRL-7988 (1964).
15. W. N. Findley, *ASTM Symposium on Plastics*, Am. Soc. Testing Materials, Philadelphia, 1944, p. 118.
16. D. L. Davies, *Statistical Methods in Research and Production*, Oliver and Boyd, London-Edinburgh, 1957.

### Résumé

La base d'une méthode statistique pour des analyses de données de rétrécissement est décrite. La méthode consiste dans la surface de réponse correspondant à l'expansion d'une série de Taylor comme une fonction autour d'un point. La méthode est capable de traiter le résultat d'extension multiaxiale et inclut d'autres variables telles que la température sans complications mathématiques impossibles. En outre, l'approche statistique peut rendre compte de telles choses, telle que l'erreur expérimentale et les variations d'échantillons. Le rétrécissement par compression uniaxiale et le comportement au recouvrement de mousse de polypropylène récemment développée, ont été mesurés sous des charges de 140 à 703 g/cm<sup>2</sup> et à des températures de 23 à 74°C. La mousse avait une densité nominale de 0.07 g/cc et un poids moléculaire moyen entre les ponts de 10.000. Le comportement est décrit par une expansion de séries de Taylor au moyen d'une fonction de second ordre en fonction de la charge appliquée, de la température d'essai, de la densité de la mousse et du logarithme du temps.

### Zusammenfassung

Die Grundlage einer statistischen Methode zur Analyse von Kriechdaten wird beschrieben. Die Methode besteht in der Anpassung der das Verhalten beschreibenden Fläche

an die Entwicklung einer Taylor'schen Reihe einer Funktion um einen Punkt. Die Methode erlaubt die Behandlung multiaxialer Spannungsdaten und umfasst weitere Variable, wie Temperatur, ohne allzu grosse mathematische Komplikationen. Weiters kann die statistische Behandlung Dinge wie, Versuchsfehler und Probenvariation berücksichtigen. Das Kriecherholungsverhalten eines neu entwickelten Polypropylenschaumstoffes bei uniaxialer Kompression wurde bei Belastungen von 140 bis 705 g/cm<sup>2</sup> und Temperaturen von 23 bis 74°C gemessen. Der Schaumstoff besass eine nominelle Dichte von 0,07 g/cc und ein mittleres Molekulargewicht zwischen Vernetzungsstellen von 10.000. Das Kriechverhalten wird mittels einer Reihenentwicklung nach Taylor durch eine Funktion zweiter Ordnung der angewendeten Belastung, Prüftemperatur, Dichte des Schaumstoffes und des log Versuchsdauer beschrieben.

Received November 18, 1966

Revised February 10, 1967

Prod. No. 1594